Joint Scheduling and Power Control for Predictable Per-Packet Reliability in URLLC

Zhibo Meng, Hongwei Zhang
Center for Wireless, Communities and Innovation, Iowa State University
{zhibom, hongwei}@iastate.edu

***Abstract*—5G-and-beyond cellular networks are set to enable ultra-reliable, low-latency communications (URLLC), catering to a wide range of applications such as real-time control and extended reality (XR). For these URLLC applications, it is crucial to ensure per-packet communication reliability and high throughput. To this end, we propose a novel joint scheduling and power control approach, denoted by PktR, that ensures application-specific per-packet communication reliability as well as high channel spatial reuse and high network throughput. PktR is designed as a close-loop system, incorporating Gain-Ratio-K (GRK) interference modeling, optimization, and transmit power control mechanisms. PktR ensures predictable interference control for receivers and fine-tunes transmit power at transmitters in a highly agile manner. Our measurement studies demonstrate for the first time the feasibility of ensuring per-packet communication reliability in live cellular systems, by showing that PktR ensures high per-packet communication SINR (e.g., 20dB) and high success probability (e.g., 0.9) across diverse network and environmental settings. Through local, distributed coordination, PktR also outperforms state-of-the-art solutions significantly. For instance, besides ensuring predictable guarantee of required per-packet communication reliability in scenarios where existing solutions are unable to provide such guarantees for up to 31.01% of the network links, PktR improves the network throughput by a factor up to 1.596.**

I. Introduction

5G-and-beyond cellular network systems are increasingly being explored for ultra-reliable, low-latency communications (URLLC) in important domains such as industrial automation [1], [2], [3]. These applications demand a high level of predictability in per-packet communication reliability to ensure that data reaches their destinations within strict timing constraints. Unpredictable packet loss introduces uncertainties in communication reliability and timeliness, and it tends to increase communication delay too, thus making it difficult to support safety-critical, real-time industrial control applications. In extended reality (XR) applications and meta-universe services [4], [5], reliable delivery of each packet enables seamless, naturalistic 3D reconstruction of real-world scenes (e.g., industrial processes), and unpredictable packet loss may well lead to uncomfortable human experience [4], [6]. While URLLC has been extensively studied in recent years, how to ensure predicable per-packet communication reliability in large-scale, multi-cell networks remains an open challenge.

This work is supported in part by the NSF awards 2130889, 2112606, 2212573, 2229654, and 2232461, NIFA award 2021- 67021-33775, and PAWR Industry Consortium.

979-8-3503-5171-2/24/$31.00 ©2024 IEEE

Major sources of packet loss in cellular systems are wireless path loss, channel fading, and co-channel interference among concurrent transmissions. Transmission power control is an effective approach to addressing wireless path loss and channel fading, and transmission scheduling is a basic mechanism to control co-channel interference. The preliminary theoretical investigation by Wang et al. [1] has highlighted the necessity of joint scheduling and power control in achieving predictable per-packet communication reliability. In particular, scheduling can be leveraged to select a set of links where the necessary communication reliability can be attained through proper transmission power control; in the meantime, transmission power control plays a crucial role in adapting to fading-induced rapid fluctuations of channel conditions. Given the non-local propagation of wireless signals in cellular networks, the scheduling and transmission power control of individual links need to be coordinated. Effective scheduling and transmission power control are challenging problems in large-scale networks by themselves individually; how to develop field-deployable joint scheduling and power control algorithms to enable predictable per-packet communication reliability in large-scale, dynamic cellular networks remains an unanswered intellectual question, not to mention real-world demonstration of running systems with guaranteed, predictably high per-packet communication reliability.

Contributions. To ensure predictable per-packet communication reliability in URLLC, we design and implement the PktR framework for joint scheduling and power control in large-scale, multi-cell networks, and we make the following contributions:

- Our PktR framework extends and transforms the preliminary theoretical insight by Wang et al. [1] into a field-deployable, two-timescale approach to joint scheduling and power control in ensuring predictable per-packet communication reliability in URLLC.
- The scheduling in PktR features the Gain-Ratio-K (GRK) interference model which is suitable for developing field-deployable distributed scheduling algorithms, and PktR schedules cellular transmissions in large-scale networks to statistically bound the receiver-side interference so that there is a feasible transmission power to ensure per-packet communication reliability along each link. PktR scheduling effectively leverages stochastic geometry and optimization to address complex interactions among

links and to predict interference dynamics for optimal transmission scheduling.
- PktR scheduling is complemented by fast-timescale, per-packet transmit power control to ensure both high network throughput and application-specific per-packet communication reliability. In particular, leveraging the Cantelli's inequality, PktR power control regulates the quantiles of receiver-side SINRs, thus ensuring the required receiver-side per-packet SINR.
- We implement PktR in the 5G open-source software platform OpenAirInterface. We experimentally validate the PktR design and implementation through the sandbox platform in the ARA wireless living lab[7], and we demonstrate for the first time the feasibility of ensuring predictable per-packet communication reliability in live cellular systems. In particular, our measurement study shows that the distributed scheduling and power control in PktR facilitates network-wide convergence, ensuring the desired per-packet communication reliability across the entire network. In addition, with local, distributed coordination alone, PktR achieves remarkable network throughput. In fact, it outperforms the state-of-the-art physical-model-based scheduler while maintaining the necessary per-packet communication reliability. For instance, besides ensuring predictable guarantee of required per-packet communication SINR in scenarios where existing solutions are unable to provide such guarantees for up to 31.01% of the network links, PktR improves the network throughput by a factor up to 1.596.

The rest of the paper is organized as follows. We summarize related work in Section II, present the system model and problem definition in Section III, present the PktR framework in Section IV, present the OAI5G-based implementation of PktR in Section V, evaluate the PktR framework in Section VI, and make concluding remarks in Section VII.

II. Related Work

A. Interference control with scheduling in wireless networks

Extensive research has been conducted on addressing interference in cellular networks. For interference control in multi-cell networks, scheduling has been studied as optimization problems where factors such as energy efficiency, spectral efficiency, user rate, and interference have been considered [8], [9], [10]. These studies, however, did not consider ensuring predictable per-packet communication reliability, and the associated solutions also required global information across networks which may well be challenging to acquire in large-scale, dynamic network settings. Machine learning (ML) methods have also been employed to address scheduling problems related to interference control [11], [12], [13]. While these approaches leverage ML to make intelligent decisions, they do not consider the specific constraints and requirements of URLLC applications. Additionally, the performance of the learned policies heavily relies on the number of training steps applied and the quality of training data. Therefore, interference control using factors optimization approach and ML methods cannot ensure the predictable per-packet communication reliability required by URLLC.

In addition to the previous approaches, interference model-based methods play a crucial role in interference control for URLLC. One such approach is presented by Feng et al. [14], where they derived a probabilistic resource allocation scheme utilizing channel statistical characteristics. Gorantla et al. [15], [16] considered the interference model where up to K links can be assigned to each subchannel in a multi-cell scenario with multiple uplink subchannels. However, the aforementioned studies utilized inaccurate interference models, resulting in degraded network capacity. Furthermore, their solutions are non-local, meaning they may not be suitable for distributed protocol design.

B. Power control in wireless networks

Power allocation has been extensively studied in URLLC. In many cases, power allocation is jointly optimized with other resource allocation methods to achieve overall performance improvements. Several studies have explored the joint optimization of power allocation with resource block assignment, blocklength, user clustering, UAV positions, and other factors. Fang et al. [17], Almekhlafi et al. [18], and Sui et al. [19] have studied joint optimization of power allocation with resource block assignment to enhance network throughput and energy consumption. Ren et al. [20] considered the joint optimization of power allocation and blocklength to minimize the decoding error probability. Elhattab et al. [21] investigated power allocation in conjunction with user clustering. These optimization-based solutions aimed to achieve optimal energy consumption, network throughput, decoding error probability, and other performance metrics while ensuring the reliability required by URLLC use cases. However, such optimization approaches often suffer from high computational complexity, as they require solving complex mathematical problems in real-time. Additionally, they tend to rely on global information, which introduces significant coordination overhead and can be challenging to obtain in dynamic network settings.

III. Preliminaries

System Model and Problem Specification. We investigate cellular networks of multiple cells, where each cell consists of a Base Station (BS) and multiple user equipment (UEs). Within each cell, there are uplinks for transmissions from UEs to the BS and downlinks for transmissions from the BS to UEs. Our network architecture aligns with existing wireless systems such as 3GPP cellular systems. In this context, a fundamental resource allocation unit is a Resource Block (RB) which represents a spectrum resource unit over a certain time slot. For instance, with the 5G numerology 1 where the subcarrier spacing is 30KHz, a RB consists of a sequence of 12 consecutive subcarriers in the frequency domain, and it can occupy a time slot of 0.5ms in the time domain.

Our study focuses on joint scheduling and power control of data transmissions at the MAC layer, with a particular

emphasis on managing interference. We consider one-hop data transmissions between close-by nodes, although the network itself is of large scale such that not every two nodes are within communicate range of one another. We focus on URLLC traffic, which has stringent reliability requirements. Given these network and traffic characteristics, our study addresses the *online slot-scheduling and power control problem*. That is, at any given time, we aim to schedule a maximal subset of links and control their transmission powers in a distributed manner, allowing for concurrent transmissions while ensuring, for each scheduled link, an application-specific lower bound on the success probability of the receiver-side SINR being no less than a threshold required by the application. Ensuring the receiver-side SINR helps ensure per-packet communication reliability, which is not only important for URLLC itself but also helps reduce the need for retransmission and thus reduce latency. Maximizing concurrent transmissions helps improve network throughput, thus helping reduce latency too [22].

As we will see in the design of PktR, its approach to joint scheduling and power control only involves distributed coordination among close-by nodes, and the approach ensures receiver-side SINR in the presence of network and environmental dynamics and uncertainties such as those in wireless channels. Therefore, PktR is applicable to large-scale wireless networks with dynamic channels. As a first step towards ensuring predictable per-packet communication reliability in multi-cell URLLC networks, we focus on scenarios where nodes are mostly immobile (e.g., in many private industrial 5G networks). For highly mobile networks, techniques such as those leveraging cyber-physical dynamics models [23] may be applied; their detailed study is an interesting future research topic. Similarly, we focus on ensuring receiver-side SINR in URLLC networks; the question of how to optimize MCS and transmission rate for a given SINR is an interesting research question but beyond the scope of this work.

Interference Model. For predictable interference control, Zhang et al. [24] have identified the Physical-Ratio-K (PRK) interference model that defines pair-wise interference relations between close-by nodes only while ensuring mean communication reliability (i.e., mean receiver-side SINR) in the presence of background noise and real-world wireless complexities such as multi-path fading and cumulative interference from all concurrent transmitters in the network. However, the PRK model [24] and existing studies on PRK-based scheduling [25], [26], [23] have mainly focused on scenarios where nodes' transmission powers are fixed even though different links can use different transmission powers. Accordingly, the PRK interference model is based on receiver-side signal and interference power, and scheduling is used to control the receiver-side cumulative interference power. Given that transmission power control directly impacts receiver-side signal and interference power and for the purpose of decoupling the impact of scheduling and transmission power control, the PRK interference model needs to be refined to be applicable to joint scheduling and power control. To this end, we observe that, give a transmitter X and a receiver R, the receiver-side signal/interference power $S_R = P_X \times G_{X,R}$, where P_X is the transmission power at X and $G_{X,R}$ is the wireless channel gain from X to R. Therefore, we propose to use a variant of the PRK model based on wireless channel gain, denoted as the *Gain-Ratio-K (GRK) model*. As shown in Figure 1, in the GRK model, given a link L between the transmitter T and its receiver R, a node C' is regarded as not interfering thus can transmit concurrently with the transmission from T to R if and only if the following holds:

$$G_{C',R} < \frac{G_{T,R}}{K_{T,R,\gamma_{T,R}}}, \tag{1}$$

where $G_{C',R}$ and $G_{T,R}$ is the average channel gain from C' and T to R, respectively. $\boldsymbol{K_{T,R,\gamma_{T,R}}}$ is the minimum real number chosen such that, in the presence of channel fading, cumulative interference from all concurrent transmitters, and power control strategies at individual links, the per-packet communication reliability required by application, $\gamma_{T,R}$, is satisfied. The GRK model defines, for each link (T, R), an exclusion region $\mathbb{E}_{T,R,\gamma_{T,R}}$ around the receiver R such that a node $C \in \mathbb{E}_{T,R,\gamma_{T,R}}$ will not transmit concurrently if and only if $G_{C,R} \geq \frac{G_{T,R}}{K_{T,R,\gamma_{T,R}}}$. As we will show in Section VI, the GRK model enables effective joint scheduling and power control for ensuring per-packet communication reliability.

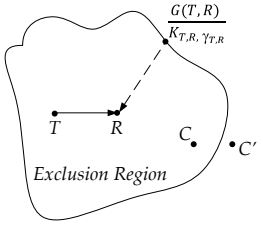

Fig. 1. GRK interference model

IV. PKTR DESIGN

A. Overview

The theoretical investigation by Wang et al. [1] has shown the necessity of joint scheduling and power control in achieving predictable per-packet communication reliability, but it left open the questions of whether it is feasible and how to develop field-deployable joint scheduling and power control algorithms that can ensure predictable per-packet communication reliability in cellular network systems using the software and hardware platforms available today. Key open challenges include complex interactions among the scheduling and transmission power control decisions across individual links, complex and fast-varying dynamics of wireless channels and interference, and real-world implementation of novel algorithms subject to the current 3GPP standards on cellular systems. We address these open systems challenges and validate the theoretical insight of Wang et al. [1] in this work.

To decouple the design of scheduling and power control policies and to decouple the interactions across different links, we leverage the two timescales of scheduling and power control decisions at the MAC and PHY layers respectively, and we propose the following framework. The adaptation of the GRK model parameter $K_{...}$ (as defined in section III) happens at a relative **slower timescale** (e.g., tens/hundreds of time

slots and at a timescale of sub-seconds/seconds) so that GRK-based transmission scheduling can control the statistics of the receiver-side interference to ensure the existence of a feasible power control strategy required for a certain per-packet communication reliability. In the meantime, the transmission power along each link is controlled on a per-packet basis and at a **timescale of milliseconds/sub-milliseconds** (e.g., each time slot) to adapt to fast-varying channel fading and instantaneous receiver-side interference.

he aforementioned framework for joint scheduling and power control is denoted as PktR and is shown in Figure 2. As the individual data packets are transmitted, receivers collect interference and channel statistics (shown as "Receiver measurement"). In the meantime, base stations collect network information such as average transmission power and path loss (shown as "Network info maintenance"). These information is used to adapt the GRK model parameter $K_{...}$ and data transmission power (shown as "K-Adaptation" and "Power control" respectively). The GRK model parameters of close-by links are shared among one another through "Protocol Signaling", and they are used to enable "TDMA scheduling" of individual packet transmissions. TDMA scheduling can use any well-established algorithm such as that from PRK-based scheduling [26], [25], and we will discuss PktR implementation details such as protocol signaling and network information maintenance in Section V. In what follows, we elaborate on the design of two key PktR components — power control and K-Adaptation.

B. IPC: per-packet instantaneous power control

Ensuring per-packet communication reliability can be translated into finding a feasible SINR regime that guarantees the delivery reliability on a per-packet basis. In particular, for a link L of transmitter T and receiver R, it can be expressed as a *success probability requirement* as follows: $Prob\{SINR_L \geqslant \gamma_{T,R}\} \geqslant \beta_L$, where $SINR_L$ is the SINR at the receiver of link L, $\gamma_{T,R}$ is the receiver-side SINR threshold to satisfy a communication reliability requirement, and β_L is a lower bound on the probability guarantee of $SINR_L \geqslant \gamma_{T,R}$ to meet the need of a given URLLC application.

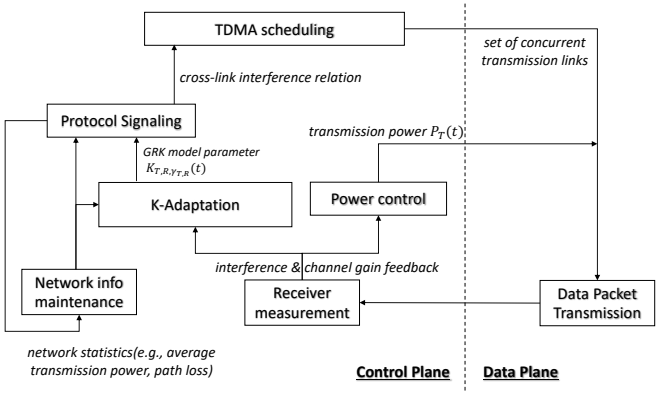

Fig. 2. PktR framework for joint scheduling and power control

Based on the mathematical analysis in our technical report [27], the success probability requirement implies the following condition:

$$P_T(t) \geqslant G_{T,R}(t) + \overline{I_R(t)} + \gamma_{T,R} + \sigma_L \sqrt{\frac{\beta_L}{1-\beta_L}}, \quad (2)$$

where $P_T(t)$ is the transmission power of the transmitter T at time instant t, $G_{T,R}(t)$ is the average channel gain between the transmitter T and receiver R, σ_L is the standard deviation of $(S_R - I_R)$ with S_R being the receiver-side data signal power, $\overline{I_R(t)}$ is the average receiver-side interference power at time instant t, and is determined by $\overline{I_R(t+1)} = c\overline{I_R(t)} + (1-c)I_R(t+1)$. The parameter c of the exponentially-weighted-moving-average (EWMA) filter in the constraint represents a weighting factor that governs the balance between stability and agility in estimating the measured interference. The term $G_{T,R}(t) + I_R(t) + \gamma_{T,R}$ is the minimum transmission power required to achieve the mean target SINR $\gamma_{T,R}$, and the term $\sigma_L \sqrt{\frac{\beta_L}{1-\beta_L}}$ is derived from Cantelli's inequality [28] to ensure the required success probability. Since higher transmission power along a link means larger interference to other links in the network and thus reduced network throughput [1], PktR uses the minimum transmission power that satisfies Inequality (2), that is, the right-hand-side (RHS) of (2), and we denote this method as *Instantaneous-reliability Power Control (IPC)*. The statistics of $G_{T,R}(t)$, I_R, and S_R in equation (2) can be collected at fast timescales, thus the IPC method enables fast-timescale, per-packet adaptation of the transmission power to in-situ channel and interference conditions.

Let P_{max} be the maximum transmission power feasible for the transmitter of link L, (2) implies the following:

$$\mathbb{E}^{max}[I_R] = P_{max} - G_{T,R}(t) - \gamma_{T,R} - \sigma_L \sqrt{\frac{\beta_L}{1-\beta_L}}, \quad (3)$$

where $\mathbb{E}^{max}[I_R]$ is the maximum expected interference power for which the PktR transmission power control can guarantee the minimum required SINR $\gamma_{T,R}$. Therefore, $\mathbb{E}^{max}[I_R]$ is a constraint when controlling receiver-side interference through the adaptation of GRK interference model.

C. K-Adaptation

Towards predictable interference control for a link L of transmitter T and receiver R, the parameter $K_{T,R,\gamma_{T,R}}$ of the GRK model needs to be instantiated according to in-situ, potentially unpredictable network and environmental conditions. In particular, if the receiver-side SINR is below (or above) $\gamma_{T,R}$, $K_{T,R,\gamma_{T,R}}$ needs to be increased (or decreased) so that the concurrent transmissions around the receiver R are decreased (or increased) accordingly, to control the receiver-side interference at an appropriate level. For convenience, we denote this mechanism as *K-Adaptation*. The choice of the GRK model parameter $K_{...}$ impacts not only the local state of a link (e.g., communication reliability) but also the overall network throughput. A link can try to increase its $K_{...}$ to increase the receiver-side SINR, but this will decrease the

network throughput. To strike an optimal balance between these competing metrics, we focus on precise control of receiver-side interference. In particular, we aim at optimal interference power control at the receiver side so as to meet the SINR requirements while maximizing concurrent communications. In what follows, we elaborate on the approach to K-Adaptation, starting with the definition of the states and their evolution equations.

State. PktR models the *in-situ instantaneous interference* at the receiver R at time instant t, denoted by $I_R(t)$, as the state variable. Then $I_R(t+1) = I_R(t) + \Delta I_R(t) + \Delta I_U(t)$, where $\Delta I_R(t)$ and $\Delta I_U(t)$ are the changes in the receiver-side interference introduced by nodes within and outside the exclusion region, respectively, due to the change of the GRK model parameter from t to $t+1$. $\Delta I_U(t)$ is treated as a disturbance to the system with mean value μ_u, and $\Delta I_U(t)$ tends to be uncorrelated with $\Delta I_R(t)$. Therefore, the time dynamics of receiver-side interference is modeled as $dI_R(t+1) = \Delta I_R(t) + \Delta I_U(t)$. In addition, we also take the β-th quantile value of the receiver side SINR $Q^{\beta}_{SINR_R(t)}$ as a state variable, and $Q^{\beta}_{SINR_R(t+1)} = Q^{\beta}_{SINR_R(t)} + \Delta SINR_R(t)$, with $\Delta SINR_R(t)$ being the change of $Q^{\beta}_{SINR_R(t)}$ due to the change of the GRK model parameter from t to $t+1$.

Control variable & cost function. Given the probabilistic nature of wireless communications, the link SINR is expected to be inherently random. Therefore, the receiver R adapts $K_{T,R,\gamma_{T,R}}$ to control $SINR(t)$ to be as close to the target SINR $\gamma_{T,R}$ as possible. In K-Adaptation, each link L with transmitter T and receiver R computes the desired change of receiver-side interference power $\Delta I_R(t)$ at a time slot t. If $\Delta I_R(t) < 0$ (or $\Delta I_R(t) > 0$), it increases (or decreases) $K_{T,R,\gamma_{T,R}}$ such that the sum of the expected interference power from all the nodes newly added to (or removed from) the exclusion region $\mathbb{ER}_{T,R,\gamma_{T,R}}$ is no less (or no more) than $|\Delta I_R(t)|$. Therefore, we treat $\Delta I_R(t)$ as the control variable of the system.

In order to control the interference to satisfy the SINR success probability requirement, the tail distribution of SINR has to be considered. From Equation (2), we know that the SINR success probability requirement implies the following condition: $\mathbb{E}[I_R(t)] \leq \mathbb{E}[S_R(t)] - \gamma_{T,R} - \sigma_L\sqrt{\frac{\beta}{1-\beta}}$, where $S_R(t)$ is the received power at time slot t. Therefore, we can treat the right-hand side of the above equation as the target interference, and try to control the expected interference $\mathbb{E}[I_R(t)]$ to be as close to the desired target as possible. More formally, the control design at time t is a model predictive control problem as follows:

$$\begin{aligned} \min \quad & (\overline{I_R(t+1)} - \mathbb{E}[S_R(t+1)] + \gamma_{T,R} + \sigma_L\sqrt{\frac{\beta}{1-\beta}})^2 \\ s.t. \quad & \overline{I_R(t+1)} = c\overline{I_R(t)} + (1-c)I_R(t+1), \end{aligned} \tag{4}$$

where $\mathbb{E}[S_R(t+1)]$ is the expected receive signal power at time slot $t+1$ (denoted by $\overline{S_R(t+1)}$), $\overline{I_R(t+1)}$ and $\overline{I_R(t)}$ are the measured average value of interference at time $t+1$ and t respectively, and $I_R(t+1)$ is the instantaneous interference power at time $t+1$. From the objective function and the constraint, we have

$$\begin{aligned} & \mathbb{E}[(\overline{I_R(t+1)} - \overline{S_R(t+1)} + \gamma_{T,R} + \sigma_L\sqrt{\frac{\beta}{1-\beta}})^2] \\ &= \mathbb{E}[(c\overline{I_R(t)} + (1-c)I_R(t+1) - \overline{S_R(t+1)} + \gamma_{T,R} + \sigma_L\sqrt{\frac{\beta}{1-\beta}})^2] \\ &= \mathbb{E}[(c\overline{I_R(t)} + (1-c)(I_R(t) + \Delta I_R(t) + \Delta I_U(t)) - \overline{S_R(t+1)} + \\ &\quad \gamma_{T,R} + \sigma_L\sqrt{\frac{\beta}{1-\beta}})^2] \\ &= \mathbb{E}[(c\overline{I_R(t)} + (1-c)(I_R(t) + \Delta I_R(t) + \mu_u) - \overline{S_R(t+1)} + \\ &\quad \gamma_{T,R} + \sigma_L\sqrt{\frac{\beta}{1-\beta}})^2]. \end{aligned}$$

We need $c\overline{I_R(t)} + (1-c)(I_R(t) + \Delta I_R(t) + \mu_u) - \overline{S_R(t+1)} + \gamma_{T,R} + \sigma_L\sqrt{\frac{\beta}{1-\beta}} = 0$ to minimize the objective. Accordingly, we have

$$\begin{aligned} \Delta I_R(t) &= \frac{\overline{S_R(t+1)} - \gamma_{T,R} - \sigma_L\sqrt{\frac{\beta}{1-\beta}} - c\overline{I_R(t)} - (1-c)I_R(t)}{1-c} - \mu_u \\ &= \frac{\overline{S_R(t+1)} - \gamma_{T,R} - \sigma_L\sqrt{\frac{\beta}{1-\beta}} - c\overline{I_R(t)} + c\overline{I_R(t-1)} - \overline{I_R(t)}}{1-c} \\ &\quad - \mu_u \\ &= \frac{\overline{S_R(t+1)} - \gamma_{T,R} - \sigma_L\sqrt{\frac{\beta}{1-\beta}} - (c+1)\overline{I_R(t)} + c\overline{I_R(t-1)}}{1-c} - \mu_u. \end{aligned} \tag{5}$$

Furthermore, we let

$$\Delta SINR_R(t) = \gamma_L - Q^{\beta_L}_{SINR_R(t)}. \tag{6}$$

Thus $\Delta SINR_R(t)$ denotes the difference between ground truth β_L-th quantile value of SINR and the target SINR.

Based on the above analysis, for a link L with transmitter T and receiver R, we develop Algorithm 1 for computing the optimal control $\Delta I_R(t)$. Firstly, each link updates its estimates of $\overline{I_R(t)}$, $\overline{I_R(t-1)}$, $\overline{S_R(t+1)}$, σ_L, and μ_u using methods similar to those in [25]. Then, base stations calculate the value of $\mathbb{E}^{max}[I_R]$. Then, base stations calculate the value of $\Delta I_R(t)$ for all links in its cell, subject to the constraint imposed by $\mathbb{E}^{max}[I_R]$ (line 5).

Algorithm 1 Compute optimal control $\Delta I_R(t)$

1: Update $\overline{I_R(t)}$, $\overline{I_R(t-1)}$, $\overline{S_R(t+1)}$ and σ_L;
2: Calculate $\mathbb{E}^{max}[I_R]$ based on (3);
3: Calculate $\Delta I_R(t)$ using (5);
4: **if** $I_R(t) + \Delta I_R(t) > \mathbb{E}^{max}[I_R]$ **then**
5: $\quad \Delta I_R(t) = \mathbb{E}^{max}[I_R] - I_R(t)$;
6: **end if**

From $\Delta I_R(t)$ to $K_{T,R,\gamma_{T,R}}(t+1)$. After the receiver R computes the control input $\Delta I_R(t)$ at time instant t according to Algorithm 1, R needs to compute $K_{T,R,\gamma_{T,R}}(t+1)$ so that, when the GRK model parameter is $\min\{K_{T,R,\gamma_{T,R}}(t), K_{T,R,\gamma_{T,R}}(t+1)\}$, the expected interference introduced to R by the nodes in either $\mathbb{ER}_{T,R,\gamma_{T,R}}(t)$ or $\mathbb{ER}_{T,R,\gamma_{T,R}}(t+1)$ but not in both is as close to $|\Delta I_R(t)|$ as

possible. To this end, we define, for each node C which may fall within the exclusion region of R, the expected interference to R as $\mathbb{E}[I_{C,R}(t)] = \mathbb{E}[\alpha_C(t)]\mathbb{E}[P_C(t)]G_{C,R}$, where $\mathbb{E}[\alpha_C(t)]$ is the expected probability for C to transmit data packets at time t, $\mathbb{E}[P_C(t)]$ is the expected transmission power at C, and $G_{C,R}$ is the average channel gain between C and R. Suppose that there are $N_{active}(t)$ number of transmitters active at time slot t with the total number of nodes N, then we have $\mathbb{E}[\alpha_C(t)] = \frac{\mathbb{E}[N_{active}(t)]}{N} = \frac{\mathbb{E}[\lambda_v^*(t)]}{\lambda}$, where λ is the node density, $\mathbb{E}[\lambda_v^*(t)]$ is the expected value of the active node intensity of the network.

Deriving the closed-form expression of $\mathbb{E}[\lambda_v^*(t)]$ falls into the domain of thinning process in stochastic geometry, which refers to a procedure where events or items are selectively removed or retained based on certain criteria.[1] In our case, the transmitters C inside the exclusive region cannot transmit concurrently with the transmitter T as shown in Figure 1, therefore, transmitters C have to be removed at time slot t, while transmitters T should be retained at time slot t. Then, we derive the intensity of the thinning process associated with GRK-based scheduling, and the calculation of $\mathbb{E}[\lambda_v^*(t)]$ is as follows:

Theorem 1. *The density λ_v^* of the thinning process of concurrent transmitters computes as follows:*

$$\mathbb{E}[\lambda_v^*] = \frac{1 - exp(-c(t+1)\lambda)}{c(t+1)}, \tag{7}$$

where $c(t+1) = \pi\mathbb{E}[d_{\mathbb{ER}}^*]^2 + (\pi l^2 + 2\pi\mathbb{E}[d_{\mathbb{ER}}^*]l) * \int_0^l \frac{2\arccos\frac{l^2+L'^2+2\mathbb{E}[d_{\mathbb{ER}}^*](t+1)*L'}{2l\mathbb{E}[d_{\mathbb{ER}}^*](t+1)+L')}}{360l} dL'$, *$l$ is the expected link length, λ is the density of the spatial Poisson process representing the cellular network under consideration, $\mathbb{E}[d_{\mathbb{ER}}^*]$ is the expected value of the radius of $\mathbb{ER}_{T,R,\gamma_{T,R}}$ at the equilibrium point.*

Proof. Proof can be found in the technical report [27]. □

GRK model adaptation. Considering the discrete nature of node distribution in space and the requirement on satisfying the minimum SINR threshold $\gamma_{T,R}$, we propose the following rule for computing $K_{T,R,\gamma_{T,R}}(t+1)$:

- When $\Delta I_R(t) = 0$, let $K_{T,R,\gamma_{T,R}}(t+1) = K_{T,R,\gamma_{T,R}}(t)$.
- When $\Delta I_R(t) < 0$, interference is not well bounded (i.e., need to expand the exclusion region), let $\mathbb{ER}_{T,R,\gamma_{T,R}}(t+1) = \mathbb{ER}_{T,R,\gamma_{T,R}}(t)$, then keep adding nodes not already in $\mathbb{ER}_{T,R,\gamma_{T,R}}(t+1)$, in the non-increasing order of their wireless channel gain to R, into $\mathbb{ER}_{T,R,\gamma_{T,R}}(t+1)$ until the node B such that adding B into $\mathbb{ER}_{T,R,\gamma_{T,R}}(t+1)$ makes $\sum_{C\in\mathbb{ER}_{T,R,\gamma_{T,R}}(t+1)\setminus\mathbb{ER}_{T,R,\gamma_{T,R}}(t)} \mathbb{E}[I(C,R,t)] \geq |\Delta I_R(t)|$ for the first time. Then let $K_{T,R,\gamma_{T,R}}(t+1) = \frac{G_{T,R}}{G_{B,R}}$.
- When $\Delta I_R(t) > 0$, we further differentiate the following situations:
  - $\Delta SINR(t) < 0$: interference is well-bounded; the exclusion region remains the same, and the transmission power is controlled to further reduce SINR towards the target.
  - $\Delta SINR(t) > 0$ and $\Delta I_R(t) > \Delta SINR(t)$: interference is over-bounded (i.e., need to shrink the exclusion region); let $\mathbb{ER}_{T,R,\gamma_{T,R}}(t+1) = \mathbb{ER}_{T,R,\gamma_{T,R}}(t)$, then keep removing nodes out of $\mathbb{ER}_{T,R,\gamma_{T,R}}(t+1)$, in the non-decreasing order of their wireless channel gain to R, until the node B such that removing any more node after removing B makes $\sum_{C\in\mathbb{ER}_{T,R,\gamma_{T,R}}(t)\setminus\mathbb{ER}_{T,R,\gamma_{T,R}}(t+1)} \mathbb{E}[I(C,R,t)] > \Delta I_R(t) - \Delta SINR(t)$ for the first time. Then let $K_{T,R,\gamma_{T,R}}(t+1) = \frac{G_{T,R}}{G_{B,R}}$.
  - $\Delta SINR(t) > 0$ and $\Delta I_R(t) < \Delta SINR(t)$: interference is well-bounded, and power control alone is enough to guarantee the SINR requirements.

[1]Even though the topology of a given network is fixed, the spatial distribution of concurrent transmitters is stochastic over time.

V. PktR Implementation

5G-compliant implementation. The PktR framework can be integrated within the existing 5G standards of the 3GPP cellular architecture. Here we present our strategy for implementing PktR in the standard-compliant, open-source 5G software platform OpenAirInterface [29]. The system architecture of PktR is depicted in Figure 3. For network information maintenance, the gNB collects data from nearby gNBs at a relatively low frequency and from UEs in the cell for every slot. The sharing of network information is achieved through protocol signaling using a real-time dedicated UDP socket. Additionally, we define a custom message "PktR-Signal" to convey the necessary information among gNBs. To incorporate the PktR framework into OpenAirInterface, we make targeted modifications to the MAC and PHY components of the platform without changing the current 5G standard. The current OAI MAC scheduling framework is composed of the downlink scheduling `nr_fr1_dlsch_preprocessor` and the uplink scheduling `nr_fr1_ulsch_preprocessor`, which are executed in the gNB, and called every slot. We extend the MAC scheduler pre-processor with PktR functions. For every period T, the gNB calculates the optimal control variable $\Delta I_R(t)$, and then utilizes the K-Adaptation mechanism to compute the GRK model parameter K for each UE within its respective cell based on the $\Delta I_R(t)$ calculated in the current period. After calculating K, gNBs share the parameter K for each UE with nearby gNBs through protocol signaling. Once the interference

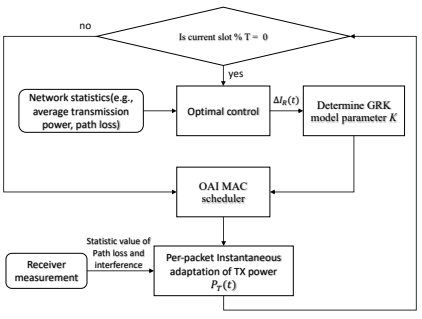

Fig. 3. PktR implementation architecture

relation is generated, PktR calls the standard-compliant uplink and downlink scheduler `pf_ul` and `pf_dl`, which implement the ONAMA scheduling algorithm [30] to make scheduling decisions. The whole computation of scheduling is based on pipelined precomputation. This means that at time instant t, all nodes calculate the status of time instant $t + M$. Therefore, when time reaches slot $t + M$, a node simply looks up the precomputed status and decides to transmit or not. In the PHY layer, the transmitters apply instantaneous power control in the function `nr_generate_pdsch` of OAI gNB and `nr_ue_ulsch_procedures` of OAI UE, using receiver measurements and control channels to determine appropriate transmission power levels. More detailed information about the PktR implementation can be found in the technical report [27]. The source code of PktR can be found at [31].

Light-weight control signaling. Control messages are used for two main purposes. The first is for BS-UE coordination. This involves real-time feedback of the receiver-side interference and the standard deviation of per-packet SINR, which are essential for determining the power control policy. It takes 4 bytes to transmit these two parameters for each transmission. The second is for inter-BS coordination. These messages contain network statistics such as the average transmission power, path loss, and exclusion region (ER) size. The control messages for updating the aforementioned statistics are exchanged at relatively low frequencies as compared with the frequency of data packet exchange, thus the incurred overhead is not high. For instance, the control message for exchanging the GRK parameter K takes 2 bytes, including the UE's ID and its corresponding parameter K. This exchange occurs only when K-adaptation happens every 30 ms. BSes also exchange information on link scheduling status required by the PktR ONAMA scheduling algorithm. At each time slot, it takes 2 bytes to exchange the scheduling status for each UE, including the UE's ID, transmission time, and transmission status. In our setting, we pre-compute 4 slots' transmission statuses. Therefore, the per-UE control message overhead for inter-BS coordination at each time slot is $8 + O(t)$ bytes, where the term $O(t)$ denotes the type of control message overhead that is incurred at rather low frequency.

Computational and energy overhead. The computational and energy overhead primarily arises from the calculations of transmission power (Equation 2), ΔI_R (Equation 5), and spatial density of concurrent transmitters (Equation 7). The calculations of transmission power and ΔI_R (i.e., Equations 2 and 5 respectively) are based on closed-form solutions, thus the per-link computational overhead tends to be low and the computational overhead at each BS is proportional to the number of nodes in the associated cell. For Equation 7, we can employ numerical integration techniques, such as the Trapezoidal Rule, to simplify the computation, effectively breaking it down into multiple closed-form solutions. Consequently, the computational overhead remains low and proportional to the number of nodes in a cell. The lightweight computation also makes the computational energy overhead low. Energy overhead is also introduced by control messages. Given the light-weight control signaling discussed earlier in the section, such control message energy overhead tends to be low too.

VI. Measurement Evaluation

We have implemented PktR in the open-source 5G software platform OpenAirInterface. Here we use the software-defined radios of the ARA sandbox [7] to validate the design and implementation of PktR with real-world systems platforms.

A. Network settings in ARA sandbox

To validate the feasibility and effectiveness of the PktR framework, we implement PktR in the 5G-compliant, 2022.w51 version of OpenAirInterface (OAI5G) and evaluate its behavior in the ARA sandbox using the USRP B210 software-defined radios (SDRs). The network consists of 28 SDRs deployed in an indoor office area of $6m \times 6.6m$. As shown in Figure 4, we uniform-randomly distribute UEs across 5 cells, with each cell containing 4 to 6 UEs. The transmission is in the time-division-duplex (TDD) mode, and we use numerology 1 with 106 physical resource blocks and 12 symbols, corresponding to a channel bandwidth of 30 MHz. The modulation schedme supported by OAI5G is QPSK; we consider three SINR thresholds of 11 dB, 14 dB, 17 dB, and 20 dB, which correspond to block error rates (BLER) of approximately 0.1, 0.05, 0.02, and 0.01 respectively. The SINR guarantee success probability threshold considered in the experiments is 0.9. Data traffic is generated using iPerf UDP packets, each 208 bytes in size. The overall network settings are shown in Table I.

Fig. 4. ARA sandbox

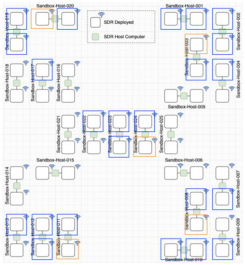

Fig. 5. ARA sandbox, with gNBs and UEs marked in orange and blue colors respectively

B. Methodology

Towards understanding the benefits of PktR in joint scheduling and power control for predictable per-packet communication reliability guarantee, we comparatively study PktR with CCSAA [15], [16], PRKS [25], and a variant of PktR. More specifically, we implement in OAI5G the following distributed scheduling protocols and comparatively study their behavior with PktR:

- *CCSAA*: The cardinality-constrained subchannel assignment algorithm (CCSAA) [15], [16] addresses the challenge of assigning up to K number of links per subchannel within a multi-cell environment. It employs the SINR

TABLE I
NETWORK SETTINGS

Network size	$6m \times 6.6m$
Number of cells	5
Number of UEs in a cell	4-6
Transmission mode	TDD
Numerology	1
Bandwidth	30MHz
Number of resource blocks	106
Number of symbols	12
Packet size	iPerf packets of 208 bytes each
MCS value and Modulation	0-9 and QPSK
SINR threshold γ	11dB, 14dB, 17dB, 20dB
SINR success probability β	0.9

interference model [24] in resource management, trying to ensure reliable communications while improving channel spatial reuse. However, CCSAA does not adaptively adjust the number of concurrent transmissions, making it difficult to ensure per-packet communication reliability in unpredictable network and environmental conditions.

- *PRKS*: PRKS [25] employs a control-theoretic approach to instantiating the PRK interference model in dynamic, uncertain network settings, and it can enable predictably high mean-link-reliability (e.g., 95%) by controlling co-channel interference in link transmission scheduling. However, PRKS does not consider joint scheduling and power control towards ensuring per-packet communication reliability.
- *GRKS with channel inversion power control (GRKS-CI)*: Same as PktR, the GRK interference model and PktR scheduling framework are used in transmission scheduling. However, power control is through the channel-inversion method, a technique employed in the 4G and 5G standards [32] where the transmit power is controlled to be inversely proportional to the channel gain. When the channel gain is low, the transmit power is increased to compensate for the weaker signal. Conversely, when the channel gain is high, the transmit power is decreased to conserve power and reduce interference to other users. GRKS-CI is used to evaluate the benefits of the IPC power control method in PktR.

C. Behavior of PktR

For the SINR requirements of 11, 14, 17, and 20 db, Figure 6 presents the boxplots illustrating the receiver-side, per-packet SINR distributions for all the links in the ARA sandbox. The 10 percentiles for the receiver SINRs are 11.98 dB, 15.03 dB, 17.87 dB, and 20.94 dB respectively. Furthermore, Figure 7 shows the detailed distributions of per-packet SINRs through the complementary cumulative distribution functions (C-CDFs). For a success probability requirement β set as 0.9, it is evident that PktR ensures the required per-packet SINR through predictable interference control and transmission power adaptation.

Figures 8 shows the GRK model parameters K for different SINR requirements. PktR achieves the desired SINR by dynamically adjusting the GRK model parameter, which directly influences the size of the exclusion region (ER) surrounding each receiver. In particular, the GRK model parameter increases alongside the SINR requirements, effectively limiting concurrent transmissions and interference from nearby nodes.

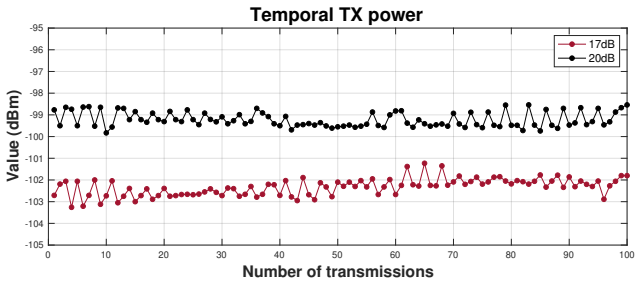

Fig. 9. Temporal TX power: $\alpha = 17, 20$

For $\gamma = 11dB$, there are 6 links whose ERs do not include all other nodes. For $\gamma = 14dB$, there are 4 links whose ERs do not include all other nodes. For $\gamma = 17dB$ and $\gamma = 20dB$, all links within the sandbox must include all the other links within their ERs, thus the parameters K are the same for the cases of $\gamma = 17dB$ and $\gamma = 20dB$. Despite this, the performance of PktR on these two cases differs due to the varying SINR distributions shown in Figure 6, which are accomplished by the power control policy shown as Figure 9. We have validated the use of Equation (7) across various settings. At $\gamma = 17dB$ and $\gamma = 20dB$, the theoretical active node intensity is 0.0354, compared to the experimental value of 0.043. At $\gamma = 14dB$, theory predicts 0.0378 versus an observed 0.045, and at $\gamma = 11dB$, the theoretical and experimental values are 0.041 and 0.046, respectively. The discrepancies between theoretical predictions and experimental results stem primarily from the model's reliance on random stochastic geometry without considering the boundary constraints, while the testbed is a fixed topology within a limited space.

Despite the distributed nature of PktR, the individual controllers converge to a state where the desired SINR is satisfied. To illustrate this behavior, Figure 10 shows the temporal evolution of the uplink SINR for a typical link when the SINR requirement is 11 dB. Initially, the link's SINR is stable around 10 dB. As other links began transmitting data, this link's SINR quickly drops to approximately 7 dB. In response, instantaneous power control increase the TX power to boost the SINR. After about 30 transmissions, K-adaptation completes, stabilizing the interference levels. Despite this stabilization, significant fluctuations in SINR during this period require continued high transmission power, maintaining elevated temporal TX power and SINR levels until around the 60th transmission. Thereafter, the transmission power gradually declines until it stabilizes around the 70th transmission, at which point the SINR also stabilizes. In our configuration, the GRK model parameter is adjusted once every three frames, or every 30 ms. This particular link transmits in every 0.5 ms uplink slot, and with each 10 ms frame containing 6 uplink slots, approximately 5 frames are required to stabilize interference.

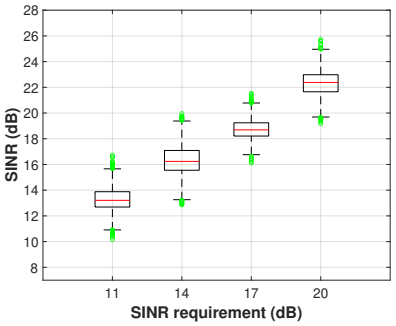

Fig. 6. Per-packet SINR

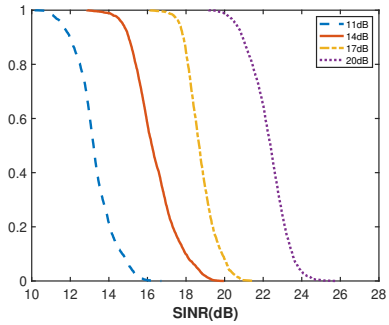

Fig. 7. Complementary CDF of Per-packet SINRs

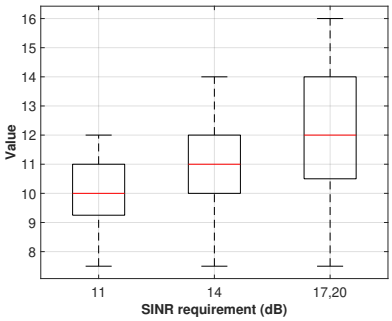

Fig. 8. GRK model parameter K

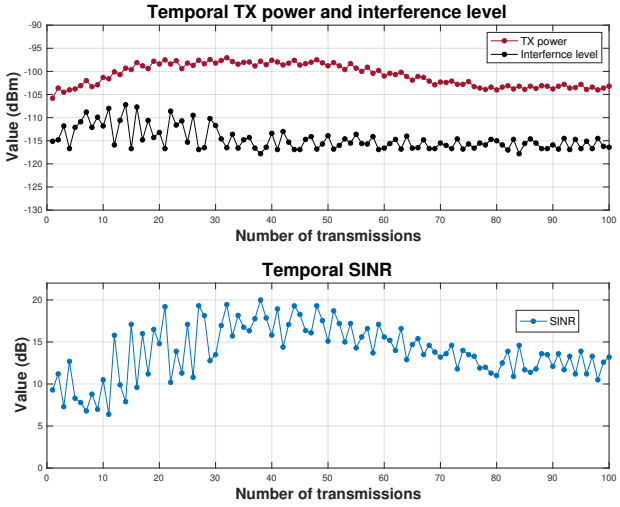

Fig. 10. Temporal link state: $\gamma = 11dB$

In general, link SINRs converge quickly in PktR, as shown in Table II, where the settling time is defined as the time

TABLE II
SETTLING TIME OF LINK SINR

SINR threshold	Mean(msec)	95% CI
γ = 11	97.24	(94.23, 100.25)
γ = 14	102.48	(98.00, 106.96)
γ = 17	107.58	(103.23, 111.93)
γ = 20	104.26	(100.87, 107.64)

required for a link to reach its steady state where SINR requirement is met. For $\gamma = 11dB$, the mean settling time is 97.24 ms with a confidence interval (CI) of $(94.23, 100.25)$. A slightly longer convergence time is observed for $\gamma = 14dB$, with a mean of 102.48 ms and a CI of $(98.00, 106.96)$, and $\gamma = 17dB$, with a mean of 107.58 ms and a CI of $(103.23, 111.93)$. This increase is attributed to the fact that, for $\gamma = 14dB$ and $\gamma = 17dB$, there are more links interfering with one another than the case of $\gamma = 11dB$, necessitating a longer duration to adjust the parameter K, which in turn extends the convergence time. Therefore, the increased ER size requires more time to achieve convergence. For $\gamma = 20dB$, the mean settling time is 104.26 ms with a CI of $(100.87, 107.64)$. Despite maintaining the similar K value as in the case of $\gamma = 17$, the larger γ reduces the value of ΔI_R. According to the K-adaptation rule, a smaller ΔI_R results in more nodes being added to the exclusion region at the same time, thereby reducing the time required for K-adaptation.

D. Comparative study

Figure 11 illustrates, for different protocols, the ratios of transmissions in which the per-packet SINR meets or exceeds the required threshold. PktR consistently achieves high satisfaction ratios for all the links in a predictable manner. They are followed by GRKS-CI, PRKS, and CCSAA. For instance, when the SINR requirement is 20dB, PktR's SINR satisfaction ratio is 96.34%, while CCSAA only achieve 31.01%. Additionally, the figure includes 95% confidence intervals for all protocols, demonstrating the stable performance of PktR across repeated experiments. In contrast, protocols such as PRKS and CCSAA fail to ensure the required per-packet SINR. This decrease in satisfaction ratio is due to the escalating levels of co-channel interference, which are not effectively managed by the PRKS and CCSAA interference models. Specifically, CCSAA schedules a fixed number of K links per subchannel during each slot and schedules concurrent links while attempting to control interference based on estimated interference. Consequently, if CCSAA schedules K links that are located far apart and cause negligible interference, their per-packet SINR is likely to be satisfied. However, when CCSAA schedules K links that result in non-negligible mutual interference, their per-packet SINR cannot be adequately fulfilled. In terms of PRKS, it only needs to satisfy the average communication reliability, resulting in a smaller ER size and increased concurrent transmissions. More specifically, Figure 12 shows the mean ER size in PRKS and PktR. PRKS has a smaller ER size, which can be attributed to the fact that PRKS only needs to guarantee the mean per-link SINR. As a result, PRKS has less stringent requirements compared to PktR, allowing for a smaller ER size. However, PktR considers Cantelli's inequality and accounts for the impact of the tail distribution when calculating the value of $\Delta I_R(t)$. While some nodes may not significantly affect the mean SINR, they can impact the per-packet SINR and reduce the SINR success probability. PktR can include such nodes in the ER, ensuring the success probability is fulfilled.

Next, we analyze the performance of the IPC policy. We observed that the per-packet SINR satisfaction ratio of PktR is higher than that of GRKS-CI. Both policies were implemented

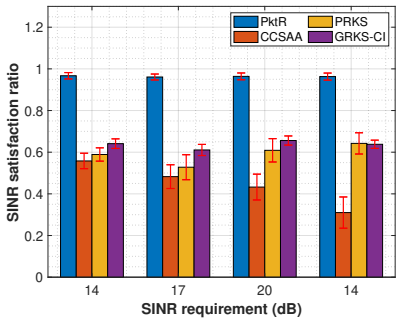

Fig. 11. SINR requirement satisfaction ratios in different protocols

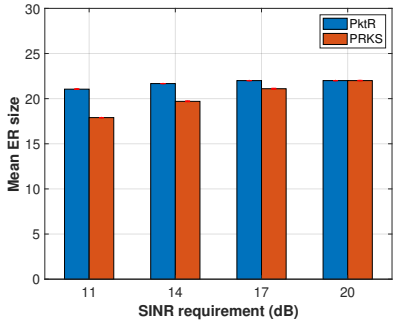

Fig. 12. Mean ER size in different protocols

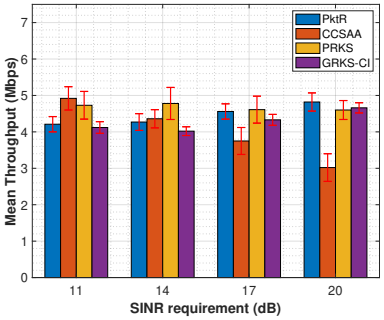

Fig. 13. Mean network throughput

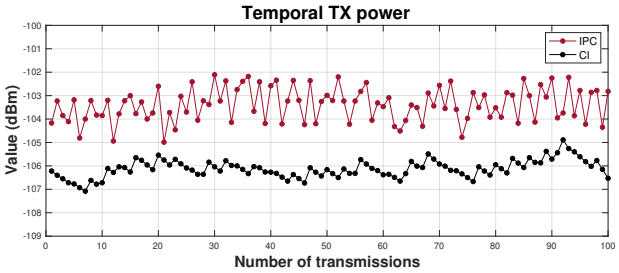

Fig. 14. Temporal transmission power: $\gamma = 11dB$

using the PktR framework for scheduling. Specifically, we compare the transmission power of IPC with that of Channel Inversion Power Control (CI) for the same receiver, as shown in Figure 14. We see that the variance of IPC is greater than that of CI. This is because the output power of IPC takes into account the feedback of instantaneous interference in addition to channel gain. As the interference varies, the output power of IPC adapts to these changes. On the other hand, CI solely considers the varying channel gain and does not take interference feedback into account. Furthermore, the overall transmission power of IPC is higher than that of CI. This can be attributed to the utilization of Cantelli's inequality in IPC (see technicical report [27]), which controls the quantile value of the transmission power. Considering that the value of σ for this time interval is approximately 0.73 and β is set at 90%, the term $\sigma\sqrt{\frac{\beta}{1-\beta}}$ in Formula (2) evaluates to 2.19. Consequently, the overall transmission power of IPC surpasses that of CI, as IPC aims to achieve a higher SINR satisfaction ratio. Based on the above observations, it is evident that CI does not control the quantiles of the transmission power and does not adjust it based on interference. As a result, the system fails to achieve a high SINR satisfaction ratio, as reflected in Figure 11.

For network throughput, Figure 13 shows the mean value of the aggregate communication throughput across all the links in different protocols. We see that PktR, GRKS-CI, and PRKS achieve similar throughput, followed by CCSAA. For instance, when the SINR requirement is 20 dB, PktR's throughput is 4.82 Mbits per second, while CCSAA only achieves 3.02 Mbits per second. Although PktR, GRKS-CI, and PRKS achieve similar throughput, their performance varies with different SINR requirements. GRKS-CI applies the same GRK interference model as PktR, resulting in similar number of concurrent transmission links to PktR. However, since CI power control cannot achieve as high SINR as PktR, the throughput is slightly lower than PktR in each scenario. PRKS achieves a much higher number of concurrent transmissions than PktR when the SINR requirement is 11 dB and 14 dB, due to its smaller ER size as shown in Figure 12. This results in a higher overall throughput, in part due to the inherent tradeoff between reliability and throughput in wireless networks [24]. As the SINR requirement increases, the overall throughput of PktR improves and surpasses other solutions for two main reasons. First, the ER size for PRKS becomes comparable to that of PktR, resulting in the same number of concurrent transmission links and transmission opportunities. Second, a higher per-packet SINR ensures a significantly stronger data signal relative to interference and noise, which leads to increased per-packet reliability and is the primary driver of throughput improvement. Since other solutions cannot achieve the same high SINR as PktR, their throughput remains lower as the SINR threshold continues to rise. The impact of high SINR on throughput is even more pronounced when advanced modulation schemes are applied, where PktR can significantly outperform other solutions. High SINR, communication reliability, and throughput help reduce communication latency, as shown by Meng et al. [22].

VII. Concluding Remarks

We have introduced the field-deployable framework PktR for ensuring predictable communication reliability in cellular networks on a per-packet basis. To maximize communication throughput while maintaining per-packet communication reliability, PktR incorporates Gain-Ratio-K (GRK) interference modeling, optimization, and transmit power control mechanisms. This comprehensive approach allows for efficient utilization of network resources. We have implemented PktR using the open-source 5G platform OpenAirInterface, and we have validated the design and implementation of PktR through extensive measurement studies using real-world hardware and the sandbox of the ARA wireless living lab. The measurement results demonstrate that PktR ensures predictably high per-packet communication reliability while achieving a high network throughput. To the best of our knowledge, this is the first work demonstrating the feasibility of ensuring predictable per-packet communication reliability in multi-cell wireless networks of real-world hardware and software systems.

REFERENCES

[1] L. Wang and H. Zhang, "Analysis of joint scheduling and power control for predictable URLLC in industrial wireless networks," in *2019 IEEE International Conference on Industrial Internet (ICII)*, 2019.

[2] Z. Meng, H. Zhang, and J. Gross, "Scheduling with probabilistic per-packet real-time guarantee for URLLC," in *arXiv*, 2023. [Online]. Available: https://arxiv.org/abs/2101.01768v7

[3] J. Baillieul and P. J. Antsaklis, "Control and communication challenges in networked real-time systems," *Proceedings of the IEEE*, vol. 95, no. 1, 2007.

[4] W. Saad, M. Bennis, and M. Chen, "A Vision of 6G Wireless Systems: Applications, Trends, Technologies, and Open Research Problems," *IEEE Network*, no. 3, 2020.

[5] F. Lamberti, F. Manuri, A. Sanna, G. Paravati, P. Pezzolla, and P. Montuschi, "Challenges, Opportunities, and Future Trends of Emerging Techniques for Augmented Reality-Based Maintenance," *IEEE Transactions on Emerging Topics in Computing*, 2014.

[6] Y. Chen, H. Zhang, N. Fisher, L. Y. Wang, and G. Yin, "Probabilistic per-packet real-time guarantees for wireless networked sensing and control," *IEEE Transactions on Industrial Informatics*, 2018.

[7] H. Zhang, Y. Guan, A. Kamal, D. Qiao, M. Zheng, A. Arora, O. Boyraz, B. Cox, T. Daniels, M. Darr *et al.*, ""ara: A wireless living lab vision for smart and connected rural communities"," in *ACM WiNTECH*, 2022.

[8] Y. Hao, Q. Ni, H. Li, and S. Hou, "Robust multi-objective optimization for EE-SE tradeoff in D2D communications underlaying heterogeneous networks," *IEEE Transactions on Communications*, 2018.

[9] Y. Zhang, H. Zhang, H. Zhou, K. Long, and G. K. Karagiannidis, "Resource allocation in terrestrial-satellite-based next generation multiple access networks with interference cooperation," *IEEE Journal on Selected Areas in Communications*, 2022.

[10] X. Zhang, T. Peng, Y. Guo, and W. Wang, "Interference-aware based resource configuration optimization for URLLC grant-free transmission," in *2023 IEEE Wireless Communications and Networking Conference (WCNC)*, 2023.

[11] J. Xu and Z. Pan, "Learning-based scheduling algorithm for D2D communication underlaying cellular networks with uncertainties," in *2022 IEEE 8th International Conference on Computer and Communications (ICCC)*, 2022.

[12] B. Khodapanah, T. Hößler, B. Yuncu, A. N. Barreto, M. Simsek, and G. Fettweis, "Coexistence management for URLLC in campus networks via deep reinforcement learning," in *2020 IEEE Wireless Communications and Networking Conference (WCNC)*, 2020.

[13] H. Yang, A. Alphones, W.-D. Zhong, C. Chen, and X. Xie, "Learning-based energy-efficient resource management by heterogeneous RF/VLC for ultra-reliable low-latency industrial iot networks," *IEEE Transactions on Industrial Informatics*, 2019.

[14] D. Feng, L. Lu, Y.-W. Yi, G. Y. Li, G. Feng, and S. Li, "Qos-aware resource allocation for device-to-device communications with channel uncertainty," *IEEE Transactions on Vehicular Technology*, 2015.

[15] B. V. R. Gorantla and N. B. Mehta, "Resource and computationally efficient subchannel allocation for D2D in multi-cell scenarios with partial and asymmetric csi," *IEEE Transactions on Wireless Communications*, 2019.

[16] B. V. R. Gorantla and Mehta, "Interplay between interference- aware resource allocation algorithm design, csi, and feedback in underlay D2D networks," *IEEE Trans. Wirel. Commun.*, 2022.

[17] C.-H. Fang, K.-T. Feng, and L.-L. Yang, "Resource allocation for URLLC service in in-band full-duplex-based v2i networks," *IEEE Transactions on Communications*, 2022.

[18] M. Almekhlafi, M. A. Arfaoui, C. Assi, and A. Ghrayeb, "Joint resource and power allocation for URLLC-eMBB traffics multiplexing in 6G wireless networks," in *ICC 2021-IEEE International Conference on Communications*, 2021.

[19] W. Sui, X. Chen, S. Zhang, Z. Jiang, and S. Xu, "Energy-efficient resource allocation with flexible frame structure for hybrid embb and URLLC services," *IEEE Transactions on Green Communications and Networking*, 2020.

[20] H. Ren, C. Pan, Y. Deng, M. Elkashlan, and A. Nallanathan, "Joint power and blocklength optimization for URLLC in a factory automation scenario," *IEEE Transactions on Wireless Communications*, 2019.

[21] M. Elhattab, M. A. Arfaoui, and C. Assi, "Joint clustering and power allocation in coordinated multipoint assisted C-NOMA cellular networks," *IEEE Transactions on Communications*, 2022.

[22] Z. Meng, H. Zhang, and J. Gross, "Scheduling with Probabilistic Per-Packet Real-Time Guarantee for Industrial URLLC," Tech. Rep. arXiv:2101.01768v7, 2024.

[23] C. Li, H. Zhang, T. Zhang, J. Rao, L. Y. Wang, and G. Yin, "Cyber-physical scheduling for predictable reliability of inter-vehicle communications," *IEEE Transactions on Vehicular Technology*, 2020.

[24] H. Zhang, X. Che, X. Liu, and X. Ju, "Adaptive instantiation of the protocol interference model in wireless networked sensing and control," *ACM Transactions on Sensor Networks (TOSN)*, 2014.

[25] H. Zhang, X. Liu, C. Li, Y. Chen, X. Che, F. Lin, L. Y. Wang, and G. Yin, "Scheduling with predictable link reliability for wireless networked control," *IEEE Transactions on Wireless Communications*, vol. 16, no. 9, pp. 6135–6150, 2017.

[26] Y. Xie, H. Zhang, and P. Ren, "Unified Scheduling for Predictable Communication Reliability in Cellular Networks with D2D Links," *Computer Communications (Elsevier)*, 2021.

[27] "Joint scheduling and power control for predictable per-packet reliability in URLLC," 2024. [Online]. Available: https://iastate.app.box.com/s/2vji8o7qjo23lezpbw5gj2e3axhxqr7c/file/1637234726030

[28] S. Boucheron, G. Lugosi, and P. Massart, "Concentration inequalities: A nonasymptotic theory of independence,(2013)."

[29] N. Nikaein, M. K. Marina, S. Manickam, A. Dawson, R. Knopp, and C. Bonnet, "OpenAirInterface: A Flexible Platform for 5G Research," *ACM SIGCOMM Computer Communication Review*, vol. 44, no. 5, pp. 33–38, 2014.

[30] X. Liu, Y. Chen, and H. Zhang, "A maximal concurrency and low latency distributed scheduling protocol for wireless sensor networks," *International Journal of Distributed Sensor Networks (Hindawi)*, no. 603172, 2015.

[31] "PktR source code." [Online]. Available: https://iastate.app.box.com/s/2vji8o7qjo23lezpbw5gj2e3axhxqr7c/file/1637241738786

[32] E. Dahlman, S. Parkvall, and J. Skold, *5G NR: The next generation wireless access technology*, 2020.